Journal of MATERIALS RESEARCH

Invited Review
DOI: 10.1557/jmr.2018.425

This section of Journal of Materials Research is reserved for papers that are reviews of literature in a given area.

UNDERSTANDING WATER-OXIDE INTERFACES TO HARNESS NEW PROCESSES AND TECHNOLOGIES

FOCUS ISSUE

Thermochemistry of volatile metal hydroxides and oxyhydroxides at elevated temperatures

Dwight L. Myers[1], Nathan S. Jacobson[2,a], Charles W. Bauschlicher, Jr.[3], Elizabeth J. Opila[4]

[1]*Department of Chemistry and Physics, East Central University, Ada, Oklahoma 74820, USA*
[2]*Materials and Structures Division, NASA Glenn Research Center, Cleveland, Ohio 44135, USA*
[3]*Thermal Protection Materials Branch, NASA Ames Research Center, Moffett Field, California 94035, USA*
[4]*Department of Materials Science and Engineering, University of Virginia, Charlottesville, Virginia 22904, USA*
[a]Address all correspondence to this author. e-mail: Nathan.S.Jacobson@nasa.gov

Received: 6 July 2018; accepted: 22 October 2018

A principal mode of corrosion in combustion or fuel cell environments is the formation of volatile hydroxides and oxyhydroxides from metal or oxide surfaces at high temperatures. It is important to determine the degree of volatility and accurate thermodynamic properties for these hydroxides. Significant gaseous metal hydroxides/oxyhydroxides are discussed, along with available experimental and theoretical methods of characterizing species and determining their thermodynamic properties.

Introduction

Reaction of metals, alloys, or oxides with water vapor at high temperatures

The reaction of water vapor with metal oxide surfaces is an extremely important area of research for a variety of engineering applications. Metal oxides can react with water vapor to produce gaseous metal hydroxides or oxyhydroxides according to the following equation:

$$\frac{1}{p}\mathrm{M}_p\mathrm{O}_q(\mathrm{s,l}) + m\mathrm{H_2O(g)} + n\mathrm{O_2(g)} = \mathrm{MO}_{\frac{q}{p}+m+2n}\mathrm{H}_{2m}(\mathrm{g}) \quad . \tag{1}$$

At higher partial pressures of H_2O, the quantity of metal hydroxide or oxyhydroxide vapor can be a significant source of material transport. Reviews by Glemser and Wendlandt [1] and Hastie [2] reported results for a variety of metallic and nonmetallic hydroxides. A previous review by Meschter et al. [3] covered an extensive portion of the periodic table. This review will focus on selected hydroxides of particular importance in water vapor/oxide interface environments such as turbomachinery and fuel cells and on the determination of reliable thermodynamic data for these species. However, basic thermodynamic data are important in many applications beyond turbomachinery and fuel cells, such as nuclear systems, materials processing, and chemical plant environments.

Combustion environments

Combustion of hydrocarbon fuels under optimal operating conditions results in a combusted gas stream containing ~3% oxygen and ~10% water vapor as well as carbon-bearing species. Thermochemistry predicts ~10% water vapor [4]; however, kinetic factors may reduce this amount to some extent [5]. Modern gas turbines may operate at higher than 1 bar total pressure, and thus, several percent water vapor would constitute a significant partial pressure. Conditions are thus conducive to water vapor/oxide reactions, which will lead to degradation of the operating surface.

Thermal barrier coatings and environmental barrier coatings in combustion environments

Metal alloy turbine blades can be engineered to withstand higher temperatures if their surface is coated with a thermal barrier coating (TBC). Refractory materials used as TBCs on turbine blades are oxides. The TBC on the surface of the turbine blade is exposed to the highest temperatures in the turbine section of the engine. A thermal gradient exists across the coating and the underlying metal alloy comprising

https://doi.org/10.1557/jmr.2018.425 Published online by Cambridge University Press

© Materials Research Society 2019

the turbine blade. State-of-the-art TBC materials are yttria-stabilized zirconia (YSZ) and most recently Gd_2O_3–ZrO_2 systems.

Environmental barrier coatings (EBCs) enable the use of light-weight high-temperature SiC or other refractory components in hot sections of high-pressure turbine engines. The combustion environments present in turbomachinery are very reactive regions in which one of the principal corrosive agents is high-temperature water vapor. In a gas turbine, the high temperature and the high pressure conditions present a very favorable environment for the formation of volatile hydroxide species. Figure 1 illustrates these portions of a gas turbine. At these pressures, species will form, which are not present in appreciable amounts in lower pressure regimes.

SiC composites have now entered service in hot section components in turbine engines, replacing some superalloy parts, due to their higher temperature capability, reduced weight, and reduced need for cooling air. SiC can form a passivating layer of SiO_2:

$$SiC(s) + 1.5O_2(g) = SiO_2(s) + CO(g) \quad . \qquad (2)$$

This layer protects against further oxidation in dry oxygen but is subject to attack by water vapor:

$$SiO_2(s) + 2H_2O(g) = Si(OH)_4(g) \quad . \qquad (3)$$

Similar reactions occurring with other constituents make study of volatile metal hydroxides imperative for understanding and preventing corrosion.

In addition to $Si(OH)_4(g)$, other volatile hydroxides and oxyhydroxides typically have higher equilibrium pressures for a given element than the simple oxide vapor species. This makes them an important mode of corrosion in many combustion systems. Aluminum oxide may also be used as a constituent of EBCs or TBCs, as well as in refractories that are exposed to high-temperature water vapor. In experiments in flowing dry oxygen atmospheres at a temperature of 1500 °C, no significant mass loss of sapphire (Al_2O_3) coupons was observed. In contrast, significant mass losses were observed in H_2O/O_2 atmospheres under the same conditions of temperature and flow rates [6, 7]. Transition metal oxides (e.g., Ta_2O_5) and rare earth oxides (e.g., Y_2O_3) may be constituents in TBCs and EBCs. These metal oxides can form volatile metal hydroxides, which will be at higher partial pressures than the corresponding oxide vapor species.

It is necessary to determine accurate thermodynamic data for the relevant hydroxides and oxyhydroxides. These data provide essential information needed to obtain reliable estimates of material loss rates under operating conditions.

Solid oxide fuel cells; steam boiler/turbine applications

Chromium steel is a prime candidate for interconnects in solid oxide fuel cells (SOFCs). High-chromium steels are desired for this application due to their ability to form electrically conductive chromium oxide, Cr_2O_3, required for cell operation in these high-temperature oxidizing environments. However, water vapor contents in the ambient air at normal relative humidity on the cathode side of the SOFC will cause significant volatilization of Cr as $CrO_2(OH)_2(g)$, poisoning solid electrolytes [8].

Oxidation of Cr in steels with concurrent volatilization of the thermally grown Cr_2O_3 from thin-walled heat exchangers/boilers/turbines leads to faster consumption of the underlying alloy and decreased component lifetimes [9]. Increasing temperatures and water vapor pressures above existing operational conditions to increase efficiency will increase the rate of volatilization of Cr_2O_3 as gaseous metal hydroxides and decrease component lifetimes. The ability to accurately predict

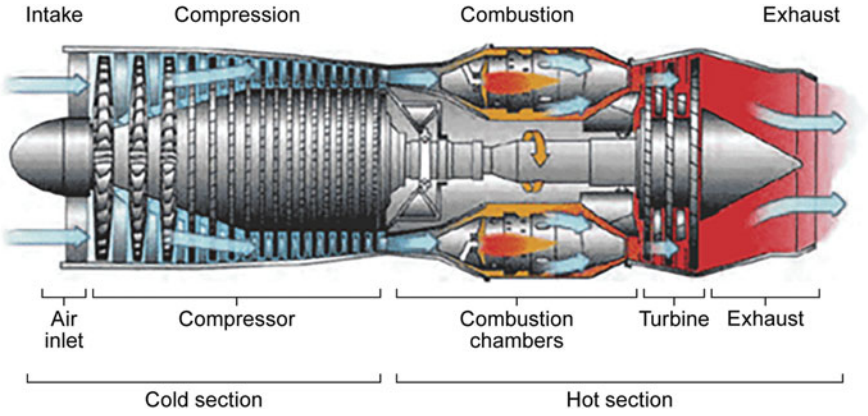


Figure 1. Schematic of a gas turbine engine. Temperatures in the turbine section can reach maximum temperatures of ~1300 °C.

https://doi.org/10.1557/jmr.2018.425 Published online by Cambridge University Press

© Materials Research Society 2019

the formation rate of these volatile species is essential to life prediction of these components.

Characterization of volatile hydroxide species

Identification of species: free jet expansion mass spectrometry

There are several ways to establish the identity of volatile hydroxide and oxyhydroxide species. One very useful technique is free jet expansion mass spectrometry. This technique allows direct sampling of a vapor stream at 1 bar total pressure. The method permits the characterization of species that are not stable or have very low pressures under vacuum conditions, as in a Knudsen effusion mass spectrometer (KEMS).

One example of such a system is shown in Fig. 2. Using an entrance orifice and a skimmer in a configuration developed by Kantrowitz and Grey [10], Milne and Greene [11], and Stearns et al. [12], an intense supersonic molecular beam is formed and directed to a quadrupole mass spectrometer. An unobstructed path to the mass spectrometer allows direct identification of vapor species formed at 1 bar while preserving their chemical and dynamic integrity. The ability to sample at 1 bar total pressure makes this system ideal for sampling combustion environments or reactive gas mixtures. The water vapor pressure regimes present in gas turbine machinery can only be studied with a mass spectrometer using this free jet expansion approach.

Recent research efforts at the NASA Glenn Research Center have centered on detection of volatile hydroxides from reaction of high-temperature water vapor with metal oxides or other materials used in combustion environments. Chemical systems that were studied include water vapor and SiO_2 [13], BN [14], Al_2O_3 [14], Ta_2O_5 [15], and Cr_2O_3 [16].

Free jet expansion sampling mass spectrometry provides positive identification of volatile species, based on mass spectra and well-understood fragmentation patterns observed in hydroxide systems. However, it is difficult to obtain quantitative data in this system because of the complex expansion process for each species in conjunction with the ionization and detection processes in the mass spectrometer. Nonetheless, some investigators have quantified this process for other high-temperature reactions [17].

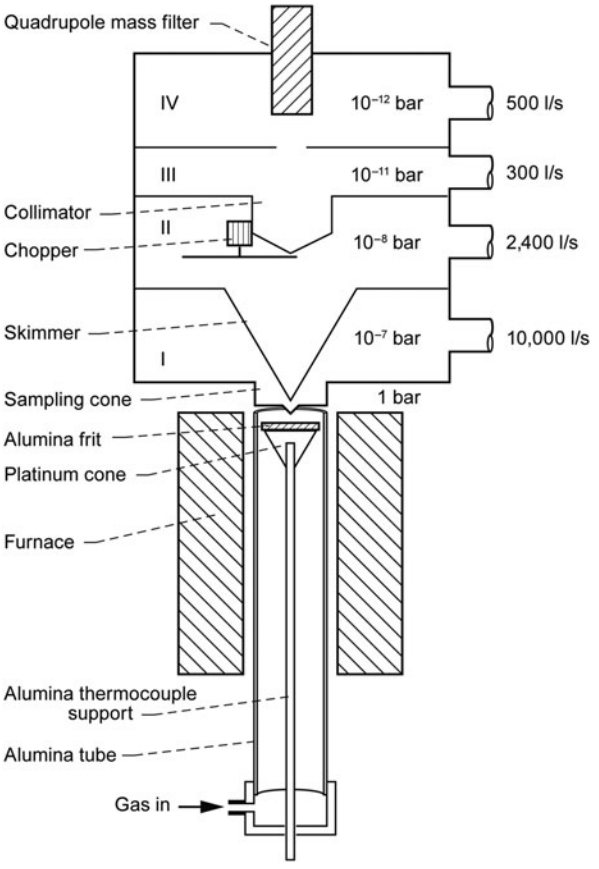


Figure 2. Schematic of free jet expansion mass spectrometer system and furnace and sample configuration. The sample (alumina or other refractory material) was situated where the alumina frit is shown.

Identification of species: dependence of flux of hydroxide species on partial pressure of water vapor and oxygen

The identity of vaporizing hydroxides can also be inferred from pressure dependency in experiments where mass transport or mass loss is measured in flowing water/carrier gas atmospheres. In thermogravimetric experiments using coupons of oxide materials, altering the partial pressure of water will alter the total mass transport of volatile hydroxide [6, 7]. A plot of log of mass transport versus log $P(H_2O)$ yields the stoichiometric coefficient for H_2O in the chemical reaction producing the

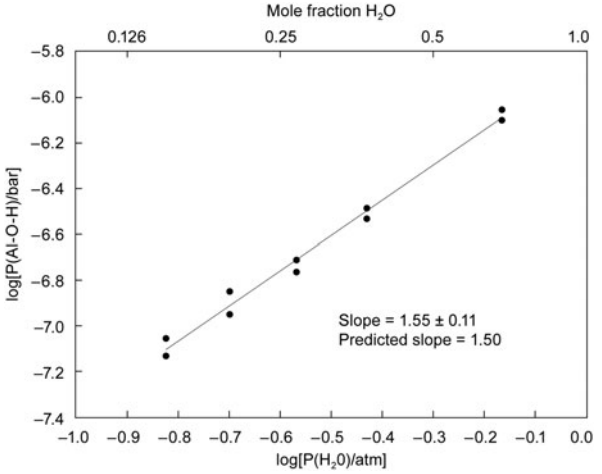


Figure 3. $P(H_2O)$ dependence on amount of $Al(OH)_3(g)$ formed. Reprinted with permission from Ref. 6. Copyright 2004 John Wiley & Sons.

https://doi.org/10.1557/jmr.2018.425 Published online by Cambridge University Press

© Materials Research Society 2019

hydroxide [see Eq. (1)]. This is illustrated in Fig. 3 for $Al(OH)_3(g)$. If there is an oxygen dependency, varying the partial pressure of oxygen will reveal it as well.

Thus, thermogravimetric analysis measurements provide evidence for the identity of reactive species by inference from the observed pressure dependence, but do not provide direct identification of molecular species. Furthermore, it is inconclusive if multiple reactions are occurring with more than one product.

Pressure dependence from transpiration measurements can also provide the species identity from inference from pressure dependence, with the same limitations. In a transpiration study of the reaction of chromium(III) oxide with oxygen and water vapor [18], Opila et al. varied the partial pressure of water and oxygen gas independently and found that the log P(Cr–O–H) versus log $P(H_2O)$ plot had a slope of 0.96 ± 0.05, while the plot of log P(Cr–O–H) versus log $P(O_2)$ had a slope of 0.77 ± 0.06 [see Figs. 4(a) and 4(b)]. The observed dependencies are consistent with the following reaction:

$$1/2Cr_2O_3(s) + H_2O(g) + 3/4O_2(g) = CrO_2(OH)_2(g) \quad . \tag{4}$$

The data indicate that the volatile species is $CrO_2(OH)_2$. The Cr–O–H transpiration study is a nice illustration of determining species identity with pressure dependence from transpiration.

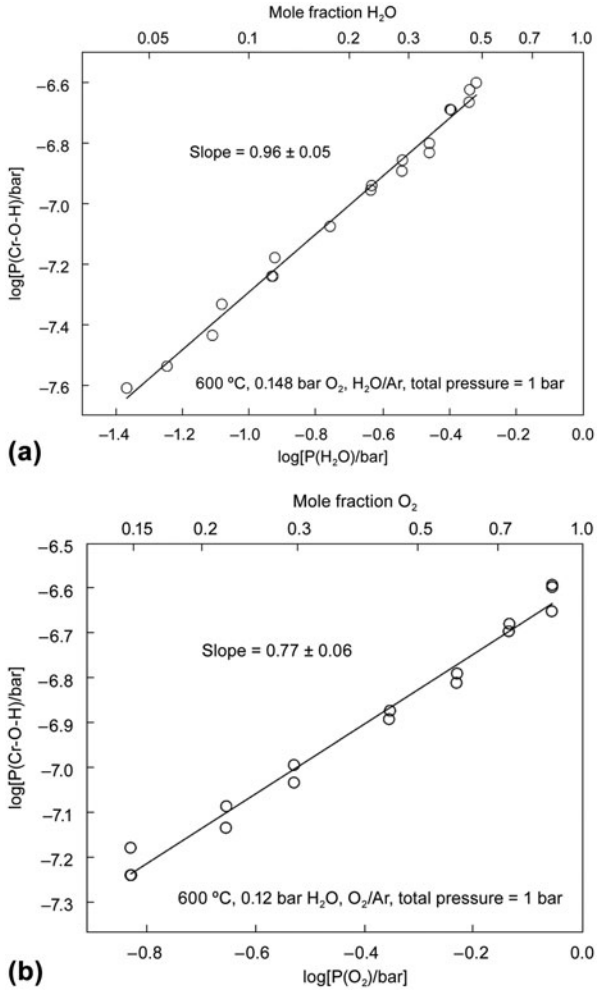


Figure 4. (a) $P(H_2O)$ dependence on amount of $CrO_2(OH)_2(g)$ formed, keeping $P(O_2)$ constant and (b) $P(O_2)$ dependence on amount of $CrO_2(OH)_2$ (g) formed, keeping $P(H_2O)$ constant. Reprinted with permission from Ref. 18. Copyright 2007 American Chemical Society.

Determination of structures and spectroscopic constants of volatile hydroxides

A knowledge of structures and vibrational frequencies is important for accurate thermodynamics. Possible methods for determining structures are (i) molecular spectroscopy [19], (ii) matrix isolation techniques coupled with spectroscopy [20, 21, 22, 23], or (iii) computational techniques [24]. Structures and vibrational frequencies are also important for determining Gibbs energy functions (gefs) if a third law analysis is performed, as discussed in section Determination of thermodynamic data.

Determination of thermodynamic data

The transpiration method—Si–O–H; Cr–O–H; Al–O–H (indirectly); Ti–O–H

The transpiration method for the determination of equilibrium pressures and reliable thermodynamic data is particularly applicable to measurements involving volatile hydroxides [1, 25, 26, 27, 28, 29, 30, 31, 32]. In this method, a gas stream flows over a sample in a boat or sample cell. Vaporized material is transported in the gas stream to a cooler region in the furnace, where it condenses in a collection tube and can be dissolved for quantitative analysis. Incorporating water vapor into the gas stream permits reaction of the oxide sample with water to produce volatile hydroxide or oxyhydroxide species. A typical configuration suitable for hydroxide studies is shown in Fig. 5.

Varying the water and oxygen vapor pressures in the gas stream will yield variation in transported material, from which the identity of the volatile species can be inferred. The results can be ambiguous when more than one reaction product is formed. Sometimes variation in temperature can lead to one species predominating in the vapor. It is essential to operate in a flow rate regime that ensures saturation of the vapor phase. Varying the flow rate establishes the region of saturation and optimal operating conditions. The equilibrium pressure of the vaporizing species is given from the following relation:

https://doi.org/10.1557/jmr.2018.425 Published online by Cambridge University Press

© Materials Research Society 2019

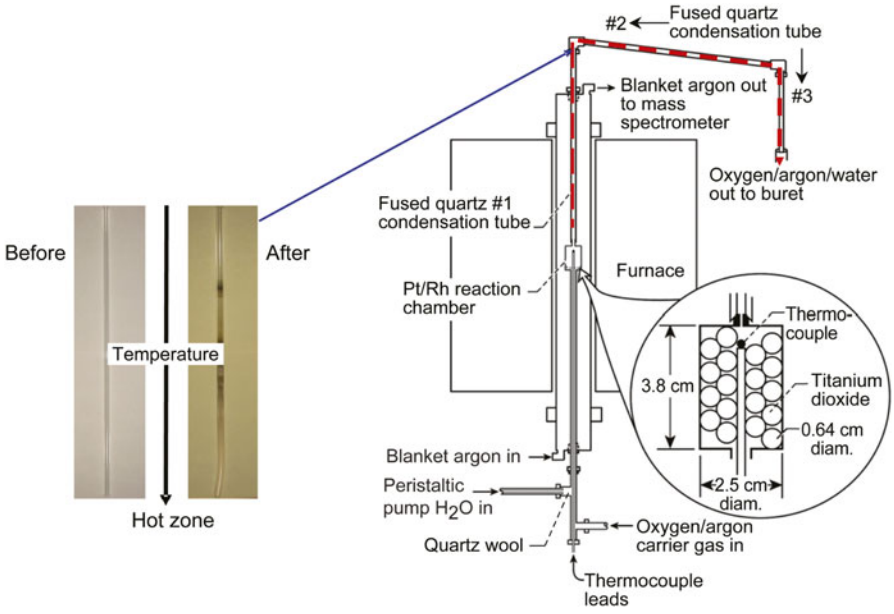


Figure 5. Transpiration furnace and transpiration cell (Pt/Rh) and (quartz) collection tubes. Insets show details of reaction chamber and condensate in the collection tubes. Reprinted with permission from Ref. 43. Copyright 2017 American Chemical Society.

$$\frac{\dot{n}_2}{\dot{n}_1} = \frac{P_2}{P_f} \quad , \tag{5}$$

where $\dot{n}_2$ and $\dot{n}_1$ are the fluxes of the volatile hydroxide species and total carrier gases, respectively, P_2 is the equilibrium pressure of the hydroxide, and P_f is the furnace pressure.

Measurement of equilibrium pressures over a range of temperatures leads to the determination of enthalpies and entropies for the reaction forming the hydroxide species, using standard methods from thermochemistry [33]. The data can be analyzed by means of the well-known second law method in which the $\ln K_p$ (K_p = equilibrium constant) for the reaction is plotted versus $1/T$ [33]. The resulting line follows the van't Hoff relation:

$$\ln K_p = -\frac{\Delta_r H^\circ}{R}\left(\frac{1}{T}\right) + \frac{\Delta_r S^\circ}{R} \quad , \tag{6}$$

$$\frac{d(\ln K_P)}{d\left(\frac{1}{T}\right)} = -\frac{\Delta_r H^\circ_{T_{av}}}{R} \quad . \tag{7}$$

Enthalpies at 298.15 K are obtained using the following expression:

$$\Delta_r H^\circ_T = \Delta_r H^\circ_{298} + \int_{298}^{T} \Delta C_P dT \quad . \tag{8}$$

The third law method [33] makes use of the gefs to compute a value of the enthalpy of reaction from each reaction temperature.

$$\text{gef}_{298.15} = \left(G^\circ_T - H^\circ_{298.15}\right)/T \quad . \tag{9}$$

This leads to the enthalpy of the reaction from Eq. (10):

$$\Delta_r H^\circ_{298.15} = T\{\Delta\{-(gef_{298.15})\} - R\ln(K_P)\} \quad , \tag{10}$$

$$\text{where : } \text{gef}_{298.15} = \left(\frac{G - H_0}{T}\right) - \left(\frac{H_{298.15} - H_0}{T}\right) = \left(\frac{G - H_{298.15}}{T}\right) \quad . \tag{11}$$

Thermodynamics of the Si–O–H system

The thermodynamics of the Si–O–H system is of great importance in a wide range of technological applications. Of particular interest is the role of high-temperature water vapor in the corrosion of ceramics that contain silicon as one component [34]. Krikorian [35] estimated thermodynamic data for several Si–O–H vapor species, including $Si(OH)_4$ and $SiO(OH)_2$. His results accurately reflect the general trends observed by experimental work which followed [31, 32]. Calculations using *ab initio* methods were performed by Darling and Schlegel [36], Allendorf et al. [37], and Plyasunov et al. [51]. Experimental measurements utilizing the transpiration method were performed by Hashimoto [31] and Jacobson et al. [32]. Hashimoto found evidence only for $Si(OH)_4$ in his transpiration experiments. Jacobson et al. found evidence for $Si(OH)_4$ and $SiO(OH)_2$ at 1673 K. A detailed assessment of all available data

https://doi.org/10.1557/jmr.2018.425 Published online by Cambridge University Press

© Materials Research Society 2019

for $Si(OH)_4$ has been given by Plyasunov [38]. Independent confirmation of the existence of the $Si(OH)_4$ and $SiO(OH)_2$ molecules was provided by Opila et al. [13] by means of free jet expansion sampling mass spectrometry. Transpiration studies can provide evidence of the vaporizing species by inference from pressure dependency of vapor transport on partial pressure of reactive carrier gases but cannot give direct observation of the vaporizing species.

The existence of $SiO(OH)_2$ in addition to $Si(OH)_4$ was inferred by Jacobson et al. [32] from vapor species pressure dependence on $P(H_2O)$; the pressure of the $Si(OH)_4$ species was subtracted out to find an equilibrium pressure of $SiO(OH)_2$. A summary of the results obtained for silicon hydroxide and silicon oxyhydroxide is given in Table I.

Thermodynamics of the Al–O–H system

Thermodynamic data for the $Al(OH)_3$ species from the reaction of water vapor with alumina were also determined by Hashimoto [31]; however, their data were measured over a two condensed phase system containing calcium monoaluminate and calcium dialuminate, rather than directly from Al_2O_3 due to difficulty of dissolving pure alumina deposits. These data have been compared with the theoretical calculations and estimates from other investigations [6, 7, 39]. A summary is given in Table II.

Thermodynamics of the Cr–O–H system

The reaction of chromium oxides with water vapor has been studied in a number of works. Ebbinghaus [40] reviewed the topic and provided data on many species. Fryburg et al. [16] used free jet expansion mass spectrometry and cooled targets to determine that the principal hydroxide species was $CrO_2(OH)_2$. Kim and Belton [30] performed transpiration experiments and reported CrO_2OH. More recently, the reaction of Cr_2O_3 with water vapor and oxygen was studied using the transpiration method by Gindorf et al. [41] and Opila et al. [18]. Because of the transport of chromium-bearing species into cooler regions of the transpiration apparatus, quartz collection tubes were used and the entire gas train and all condensed water was collected and analyzed for Cr using ICP. Enthalpies of formation as determined in this study are given in Table III. Using this technique, Belton and coworkers studied hydroxides of W [27] and Mo [28].

Thermodynamics of the Ti–O–H system

An extensive study utilizing both experimental (transpiration) and computational approaches was performed by Nguyen et al. [42, 43]. Their experiments utilized the reaction of water vapor with TiO_2 (rutile). The predominant reaction was determined to be:

$$TiO_2(s, \text{rutile}) + H_2O(g) \rightleftharpoons TiO(OH)_2(g) \quad . \qquad (12)$$

Some evidence was also found for the formation of $Ti(OH)_4$, according to the following reaction:

$$TiO_2(s, \text{rutile}) + 2H_2O(g) \rightleftharpoons Ti(OH)_4(g) \quad . \qquad (13)$$

Accurate computational results for both species were determined [43]. The recommended values from their study are listed in Table IV.

Laminar flow methods—Al–O–H; Ta–O–H

Reactions of water vapor with refractory oxides can also be studied using mass losses from oxide coupons under laminar flow conditions. In this technique, sample coupons are suspended from a recording balance in a tube furnace and the reactive gas mixture flows over them, as shown in Fig. 6. Due to the approximations necessary to derive diffusion-limited reaction rates, such an experiment cannot be used to obtain precise thermodynamic data. Nonetheless, it is a quick and relatively easy screening method for different systems.

A schematic representation of the volatilization process is illustrated in Fig. 7, with SiO_2 as substrate and $Si(OH)_4$ as the volatile species. As in the transpiration method, the nature of the volatile species is inferred from partial pressure

TABLE I. Values obtained for $Si(OH)_4$ and $SiO(OH)_2$.

Species	Reference	$\Delta_f H°(298)$ (kJ/mol)	S°(298) (J/mol-K)	Comments
$Si(OH)_4$	Allendorf et al. [37]	−1342.2 ± 13.8	342.54	Ab initio
	Jacobson et al. [32]	−1351.3 ± 1.7	...	Transpiration
	Hashimoto [31]	−1355.0 ± 1.5	348.3	Transpiration
	Plyasunov [38]	−1340.68 ± 6.2	...	...
	Plyasunov [51]	−1346.30 ± 2.37	338.550 ± 1.32	Ab initio
$SiO(OH)_2$	Jacobson et al. [32]	−836 ± 40	...	Transpiration

$\frac{C_p}{R} = 27.4945 - 6.22157 \times 10^{-3}T + 4.34739 \times 10^{-6}T^2 - 9.07719 \times 10^{-10}T^3 - 4.48699 \times 10^{3}T^{-1} + 2.58937 \times 10^{5}T^{-2}$ (T = 298.15–2100K) [51].

https://doi.org/10.1557/jmr.2018.425 Published online by Cambridge University Press

© Materials Research Society 2019

TABLE II. Values obtained for $Al(OH)_3$.

Reference	$\Delta_f H°(298)$ (kJ/mol)	S°(298) (J/mol-K)
Gurvich et al. [39]	−1012 ± 50	301.535
Hashimoto [31]	−1004.2 ± 15.0	313.8 ± 7.9
Opila and Myers [6]	−1008.6 ± 11 (1650 K)	...

From Refs. 39 and 57.
C_p (J/mol-K) = 74.511990 + 9.545527 × $10^{-2}T$−4.112512 × $10^{-5}T^2$−1075464.0T^{-2} (298–700 K).
C_p (J/mol-K) = 109.1773 + 2.979339 × $10^{-2}T$−5.317581 × $10^{-6}T^2$−4138997T^{-2} (700–2400 K).
C_p (J/mol-K) = 153.8085 + 1.120288 × $10^{-3}T$−8.592387 × $10^{-8}T^2$−38406420T^{-2} (2400–6000 K).

TABLE III. Values obtained for $CrO_2(OH)_2$.

Method	$\Delta_f H°$ (kJ/mol)	S° (J/mol-K)
Second law experiment [18]	−758 ± 7 (861 K)	337.6 ± 16.4 (298 K)
Using C_p [18]	−760 ± 7 (298 K)	...
Using C_p, Ebbinghaus [18, 40]	−760 ± 7 (298 K)	...
Third law experiment and gef from Ref. [18]	−776 ± 6 (298 K)	...
Ab initio calculation CCSD(T) from Ref. [18]	−792 ± 20[a] (298 K)	317.9 ± 10 (298 K)

[a]Calculated from the isogyric reaction: $CrO_2(OH)_2(g) \rightarrow CrO_3(g) + H_2O(g)$.
C_p (J/mol-K) = 163.4872 − 0.015289T + 3.57 × $10^{-6}T^2$ − 18249.2T^{-1} − 1.94 × $10^{-10}T^{-2}$ (298–1000 K).

TABLE IV. Values obtained for $TiO(OH)_2$ and $Ti(OH)_4$ [43].

Species	Method	$\Delta_f H°$ (298) (kJ/mol)	S° (298) (J/mol-K)
$TiO(OH)_2$	Second law experiment	−937.8 ± 15	320.67
	Third law experiment	−838.9 ± 6.5	...
	Theoretical B3LYP DFT CCSD(T)	−839 ± 25[a]	...
$Ti(OH)_4$	Theoretical B3LYP DFT CCSD(T)	−1274 ± 21[b]	373.7

[a]Calculated from the reaction $Ti(g) + O_2(g) + H_2O(g) \rightarrow TiO(OH)_2(g)$
[b]Calculated from the reaction $Ti(g) + O_2(g) + 2H_2O(g) \rightarrow Ti(OH)_4(g)$
For $TiO(OH)_2$, $C_P(298-1600\ K)(J/mol\text{-}K) = 149.2 + (-0.02539)T + (8.28697 \times 10^{-6})T^2 + \frac{-15614.05}{T} + \frac{-5.2182 \times 10^{-11}}{T^2}$ J/mol K.
For $Ti(OH)_4$, $C_P(298-1600\ K)(J/mol\text{-}K) = 169.25 + (-7.1896 \times 10^{-3})T + (7.5164 \times 10^{-6})T^2 + \frac{-10818.0308}{T} + \frac{-4.8145 \times 10^{-11}}{T^2}$ J/mol K.

dependencies. Mass losses of the sample coupons are readily related to the partial pressures of the reactive gases, e.g., H_2O and O_2. The pressure dependence of the flux yields the stoichiometry of the chemical reaction. A diagram of the water vapor thermogravimetric apparatus (TGA) is shown in Fig. 6. Under laminar flow conditions, the reaction produces a flux of volatile reaction species as shown in Fig. 7. The equilibrium pressures are related to mass fluxes (unit mass per unit time, $\Delta w/\Delta t$) and reaction characteristics by the following equation [44]:

$$\frac{\Delta w}{\Delta t} = 0.664\left(\frac{\rho' v L}{\eta}\right)^{1/2}\left(\frac{\eta}{\rho' D}\right)^{1/3}\left(\frac{DPM}{LRT}\right) \quad . \qquad (14)$$

Where ρ' is the gas density of the boundary layer, v is the gas velocity, η is the gas viscosity of the boundary layer, L is the characteristic length of the sample, D is the interdiffusion coefficient of the reactive gaseous species in the laminar boundary layer, P is the partial pressure of the volatile species, M is its molar mass, R is the ideal gas law constant, and T is the temperature. From this relation, equilibrium pressures may be calculated, or given measured pressures, expected mass losses may be calculated under known flow rates.

Formation of $Al(OH)_3(g)$

A study of the reaction of alumina with water vapor utilizing this technique was performed by Opila and Myers [6]. In their experiments, sapphire coupons were exposed to flowing streams of water vapor/oxygen gas at temperatures between 1250 °C and 1500 °C, and water vapor partial pressures between 0.15 and 0.68 atm. Linear gas velocities of 4.4 cm/s were used in fused quartz tubes of diameter 2.2 cm, which gave laminar flow conditions. The results were used to calculate equilibrium pressures of $Al(OH)_3$ from the following reaction:

$$1/2Al_2O_3(s) + 3/2H_2O(g) \rightleftharpoons Al(OH)_3(g) \quad . \qquad (15)$$

In these experiments, good agreement with Hashimoto's data for $Al(OH)_3$ [31] were obtained. An important aspect of this study in relation to that of Hashimoto is that the reaction of alumina with water was observed directly as opposed to measurements over a two condensed phase mixture of calcium aluminates. The dependency of partial pressure of water vapor on mass loss was found to be 1.55 ± 0.11, consistent with reaction [Eq. (15)] above. In addition, the results provided reliable recession rates for alumina in water vapor streams [7].

Formation of Ta–O–H species

A similar study of the reaction of tantalum(V) oxide in water vapor was performed by Myers et al. [15]. Evidence for significant mass losses from tantalum(V) oxide in 50% H_2O streams was observed. Coupons of Ta_2O_5 were suspended in a TGA apparatus similar to the one used by Opila and Myers [6]. Mass flux dependence of vaporizing Ta–O–H species were determined at 1250 °C and at 1450 °C. At 1250 °C, the slope was determined to be 2.37 ± 0.35; at the higher temperature, the slope was 2.13 ± 0.15. At the lower temperature, the slope is consistent within experimental error with the reaction:

https://doi.org/10.1557/jmr.2018.425 Published online by Cambridge University Press

© Materials Research Society 2019

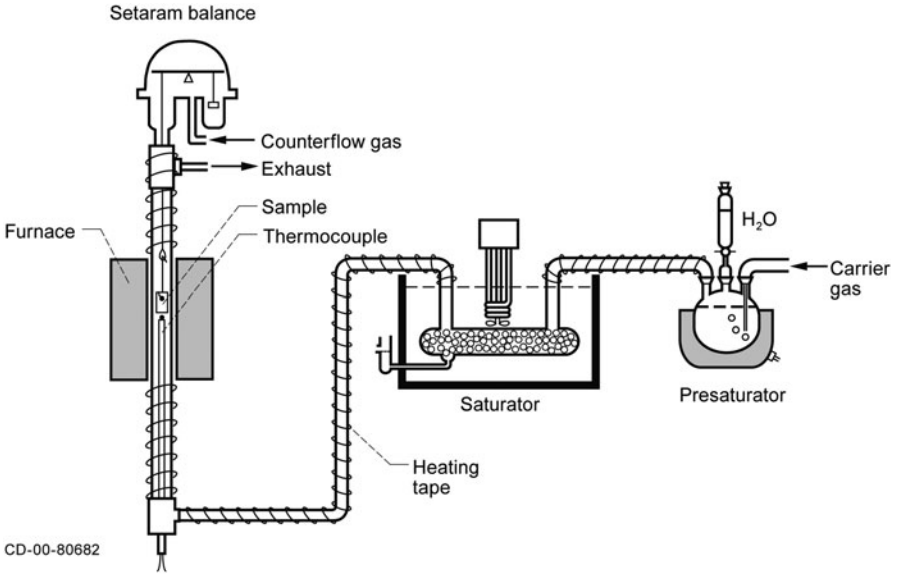


Figure 6. Schematic of thermogravimetric apparatus used to study reactions of ceramic oxide coupons with moist atmospheres. Partial pressure of water vapor in gas stream is set by the temperature of the water bath in the saturator. A counterflow of gas is necessary to prevent condensation of volatile species or moisture on the electronic balance.

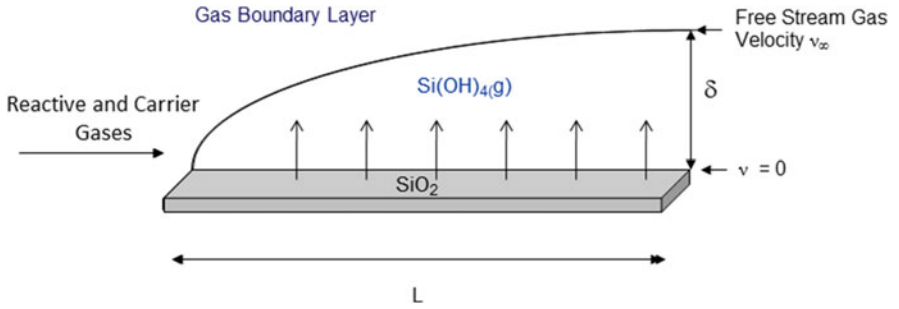


Figure 7. Schematic of volatilization process from a surface experiencing laminar flow of a reactive gas. In the example, the reactive gas is water vapor and the surface is silica.

$$1/2Ta_2O_5 + 5/2H_2O \rightleftharpoons Ta(OH)_5 \quad . \qquad (16)$$

At the higher temperature, the observed slope may be the result of competing vaporization reactions, possibly Eq. (16) and the reaction to produce $TaO(OH)_3$:

$$1/2Ta_2O_5 + 3/2H_2O \rightleftharpoons TaO(OH)_3 \quad . \qquad (17)$$

Free jet expansion mass spectrometry results found evidence for $TaO(OH)_2^+$, which would be the expected fragmentation product from $TaO(OH)_3$. No clear evidence of $Ta(OH)_5$ was found in mass spectrometric measurements. Measurements were performed in a 50% H_2O–Ar atmosphere, and substantial mass losses were observed from 70% dense Ta_2O_5 coupons. Mass losses at temperatures of 1350 °C and higher were observed to be greater than those observed from SiO_2

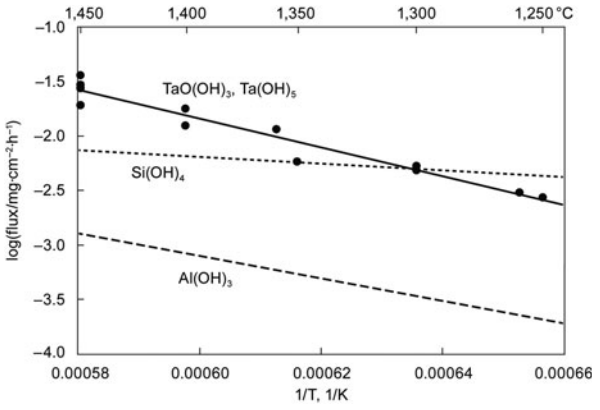


Figure 8. Measured weight loss fluxes of oxides due to volatile hydroxide and oxyhydroxide formation. Ta_2O_5 is compared with calculated fluxes from hydroxides of SiO_2 and Al_2O_3 in 50% H_2O–Ar at 1 bar total pressure and 4.4 cm/s linear flow rate. Reprinted with permission from Ref. 15. Copyright 2017 John Wiley and Sons.

https://doi.org/10.1557/jmr.2018.425 Published online by Cambridge University Press

© Materials Research Society 2019

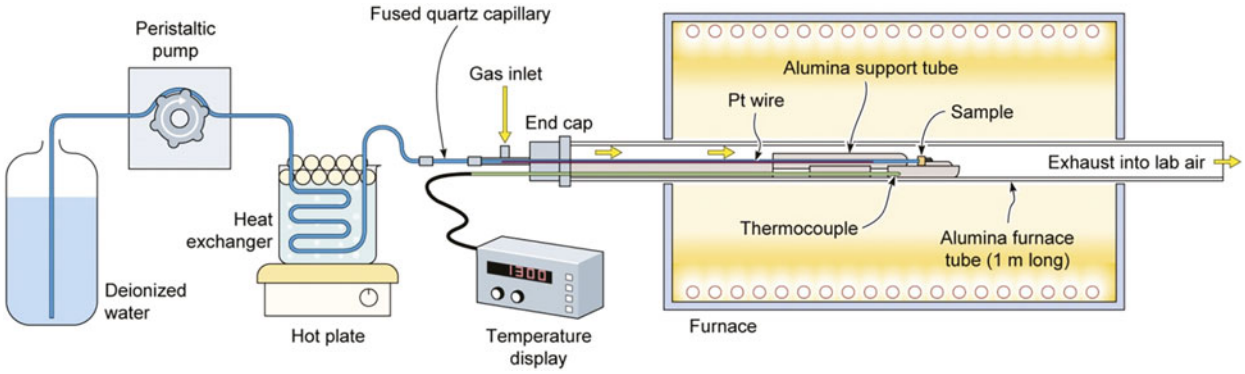


Figure 9. Steam jet furnace schematic. Reprinted with permission from Ref. 46. Copyright 2016 Elsevier.

under the same conditions. A plot of predicted equilibrium fluxes of tantalum species versus $1/T$ is shown in Fig. 8, along with pressures of $Si(OH)_4$ and $Al(OH)_3$ for comparison.

The steam jet

An additional technique for quantifying reactions of water vapor with refractory oxides utilizes a high-velocity jet of steam formed in a tube furnace [45, 46]. As shown in Fig. 9, liquid water is injected into a small-diameter capillary contained within a tube furnace. As the liquid enters the hot zone of the furnace and vaporizes, the resulting volume expansion forces the steam out of the capillary at high velocities. Sample coupons are placed in close proximity (1 mm) to the high-velocity jet of steam (150–250 m/s), allowing the reactive gas mixture to flow over the test specimen. Recession of the oxide is a direct result of the reaction and recession rates can be directly correlated with the equilibrium partial pressure of the relevant gaseous metal hydroxides. Figure 10(a) shows the measured recession profile of single crystal Al_2O_3. Figure 10(b) shows a side-by-side comparison of the measured recession of SiO_2 and Al_2O_3 with the partial pressures of $Si(OH)_4(g)$ and $Al(OH)_3(g)$, showing the measured recession correlates with the partial pressure of the volatile species as expected from Eq. (14). Recent work has focused on extending this work to study volatility of Ta_2O_5 and TiO_2. The steam jet recession of Ta_2O_5 was found to be consistent with the TGA results cited above when accounting for differences in temperature, water vapor partial pressure, and gas velocity (laminar flow), and assuming that the $TaO(OH)_3(g)$ species was the relevant species of interest [47].

Theoretical computation of thermodynamic data for volatile hydroxides

Historical: estimates

Krikorian [35, 48] estimated volatilities of a wide range of metal hydroxides, based on periodic trends and existing spectroscopic and thermodynamic data. Estimates of vibrational frequencies and molecular geometries were drawn from similar molecules. His work was very insightful and showed considerable intuition. Subsequent experiments have shown his estimates to be quite accurate in many cases, and they still fill in many gaps in the experimental literature. Today, they are a useful point of comparison for experimental and theoretical work in the field.

Accurate determination of molecular structure and vibrational frequencies

To obtain accurate third law analyses of thermodynamic data requires reliable determinations of the structure and vibrational frequencies of the hydroxide molecules in question. Historically, structures of gaseous molecules have been obtained from microwave spectroscopy or electron diffraction [49], while vibrational frequencies have been determined from infrared and/or Raman spectroscopy [19]. These methods require a significant equilibrium vapor pressure of the species of interest in the optical path of the spectrometer. Since many of the species of interest have relatively low equilibrium pressures, it is difficult or impossible to make such measurements using traditional spectroscopic techniques. This means that for many species of interest, only second law analyses can be performed on the experimental data unless an alternate method of determining structures and vibrational frequencies can be found.

Computation of gefs

Using modern ab initio methods, structures and gefs can be determined for molecules of interest. These methods are sometimes the only source of structure and vibrational frequencies of these molecules. This approach has been used to perform third law analyses on $Si(OH)_4$ by Jacobson et al. [32], using the ab initio calculations of Allendorf et al. [37]. Hashimoto [31] used data from Gurvich et al. [39] for his third law analysis of his $Al(OH)_3$ data and from the JANAF Tables [50] for $Ca(OH)_2$.

https://doi.org/10.1557/jmr.2018.425 Published online by Cambridge University Press

© Materials Research Society 2019

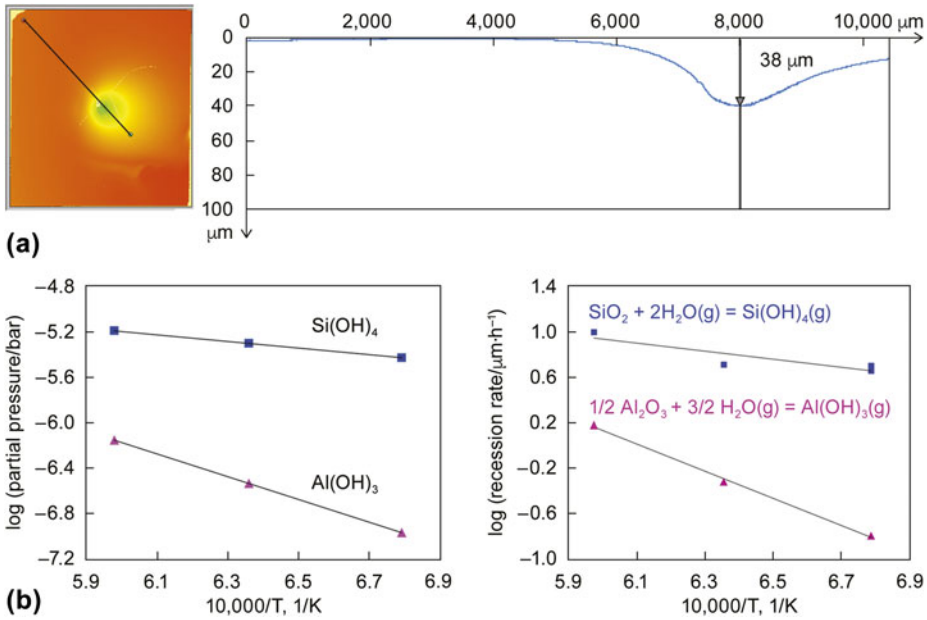


Figure 10. (a) Measured recession profile of single-crystal Al_2O_3 exposed to steam jet. The Al_2O_3 recession was measured after exposure at 1400 C, 1 bar $P(H_2O)$, 176 m/s steam velocity for 25 h. (b) Side-by-side comparison of the calculated pressures of $Si(OH)_4(g)$ and $Al(OH)_3(g)$ versus 1/T with the measured recession of SiO_2 and Al_2O_3.

Computational determination of accurate thermodynamic properties

Thermodynamic data may be computed to a high degree of accuracy using composite methods [24]. Recently, Plyasunov et al. [51] have reported computed thermodynamic data for the $Si(OH)_4(g)$ species, which is consistent with experiments and prior computations. Theoretical and experimental results are best reported as part of the same study and together can provide a reliable dataset. Opila et al. reported both experimental and theoretical results for the Cr–O–H system [18]; Nguyen et al. reported both experimental and theoretical results for the Ti–O–H system [43].

Computational chemistry can make two contributions to the determination of thermodynamic properties. The first is in the determination of the structure and vibrational spectra of the molecules of interest, which allows the determination of the temperature dependence of the thermodynamic properties. This allows the extrapolation of high-temperature experimental properties to lower temperatures. The second is by directly computing atomization or bond energies, which can be combined with known heats of formation, to determine the properties of the compound of interest.

The advent of analytic first and second derivatives for many types of computational methods, including density functional theory (DFT) approaches, makes it possible to optimize the geometry and determine the harmonic frequencies of even large molecules [52]. Experience has shown that the B3LYP hybrid functional yields very reliable structures and vibrational frequencies [53]. Scaling of the computed harmonic frequencies has been shown to account for basis set incompleteness and anharmonic effects. For many molecules, the rigid rotor-harmonic oscillator approximation can be used to compute the temperature dependence of the thermodynamic functions. However, for the metal hydroxides, the OH rotational barrier is rather low, meaning that this motion does not behave like a harmonic oscillator, but rather like a hindered rotor. This commonly occurs in organic molecules, for example, the rotation of $-CH_3$ groups [54]. As a result, excellent approximations have been developed to treat such rotations, requiring only the calculation of the rotational potential [53]. The metal oxides have an additional problem in that the MOH bending potential is very anharmonic and even have a double-well potential in some cases [43]. This arises because the M–OH bonding is a mixture of covalent, which favors a bent geometry, and ionic bonding, which favors a linear geometry. We treat this problem by computing the MOH bending potential and evaluating many vibrational levels, which are then used to compute the thermodynamic properties as a function of temperature. Thus, while metal hydroxides require one to go beyond the rigid rotor-harmonic oscillator approximation, the corrections are straight forward and can be determined using potentials computed at the same level of theory as the geometry and harmonic frequencies.

To accurately compute the heats of formation requires a rigorous computational method. The coupled-cluster singles and doubles approach with a perturbational treatment of the triple excitations [i.e., CCSD(T)] has proven to be the method of choice. The CCSD(T) treatment can be performed in

https://doi.org/10.1557/jmr.2018.425 Published online by Cambridge University Press

© Materials Research Society 2019

a series of one particle basis sets and the results extrapolated to the complete basis set limit. It should be noted that for larger systems, this method will become prohibitively expensive, and hybrid methods have been developed, where the CCSD(T) results obtained in a small basis set are corrected for basis set incompleteness using lower levels of theory. For small molecules containing only atoms from the first and second rows of the periodic table, computational chemistry has proven that it can rival all but the very best experiments. For the metal hydroxide systems, the calculations are more difficult and the accuracy is probably somewhat lower, but the computed values are an excellent check on the experimental values.

Future directions of research

Much remains to be determined in the area of volatile hydroxides of interest in high-temperature corrosion environments. More accurate data are needed for a number of chemical systems.

Figure 11 shows the periodic table with known hydroxide compounds. A recent review includes a summary of the data available [3]. The shaded elements indicate that thermodynamic data are known or needed. The blue shade indicates that the data are fairly well known. Note this includes the main Group I and II hydroxides, and these data are listed in the common data compendia [39, 50]. Generally data are not available for the transition metal hydroxides and oxyhydroxides, with the exception of Ti, Cr, Mo, and W. The data for Fe, Ni, and Co appear to be good, but limited. Chromia is an important protective oxide and Mo and W are used in the lighting industry and as structural refractory materials in reducing environments. Data are also available for the hydroxides and oxyhydroxides of B, Al, and Si. We have indicated formulae for the molecules that are known. Beyond these distinct groups, data are limited.

Refractory oxides are an important class of materials, which may also be used in environments where steam is encountered. Refractory bricks and refractory oxide coatings are important applications in steam-containing environments. As noted, data are available for some of the components of these materials—Al_2O_3, SiO_2, MgO, and CaO. However, for the more exotic constituents, such as the rare earth oxides, few data are available.

As described earlier, Krikorian [48] estimated thermochemical data for several rare earth hydroxides and oxyhydroxides. His data give very low partial pressure for species such as $Y(OH)_3(g)$, which is consistent with the well-known stability of YSZ in combustion environments over long times. More recently, Courcot et al. [55, 56] have conducted volatility measures of rare earth oxides in high-temperature water vapor. They report higher vapor pressures, which are not consistent with Kirkorian's estimates or practical experience with rare earth oxides in environments with water vapor. Preliminary steam jet results are in agreement with those of Krikorian, indicating Y_2O_3 is extremely stable in high-temperature steam. Clearly, this inconsistency should be resolved.

The authors have promoted a combined computational/experimental approach to obtain the required thermodynamic data. As noted, availability and expertise in computational methods are growing rapidly, and it is now feasible to compute the desired data for many of these complex hydroxides and oxyhydroxides. Experiments provide quantities derived from actual conditions close to the actual applications. A judicious choice of theoretical approaches and appropriate experiments can generate a reliable dataset, which is needed for many of the transition metal and rare earth hydroxides and oxyhydroxides.

The experimental methods discussed here—both the traditional ones such as transpiration, thermogravimetric

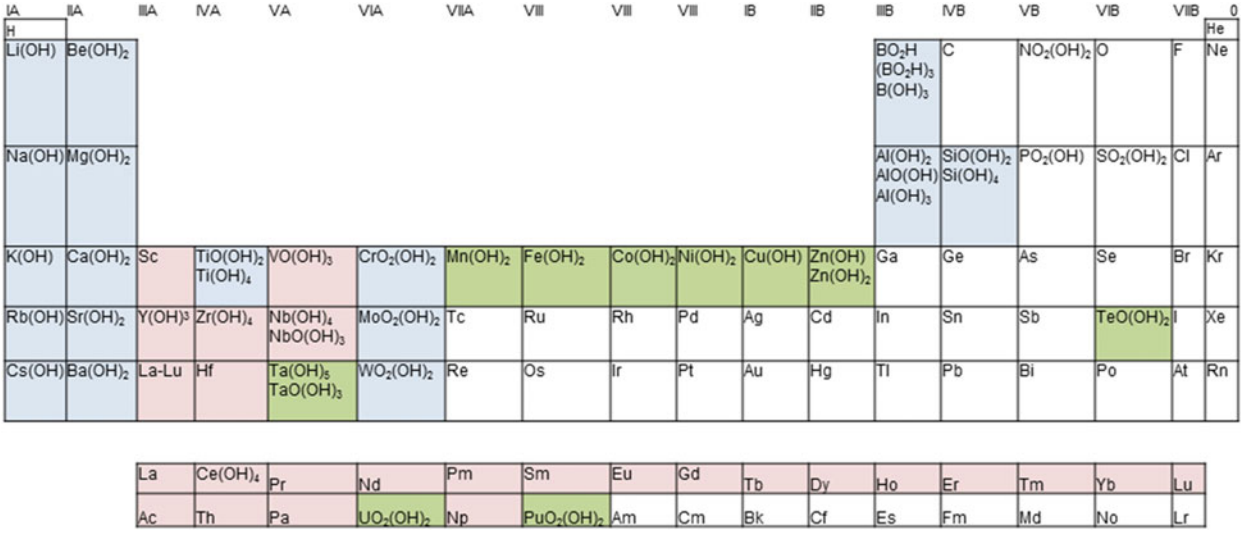


Figure 11. Periodic table illustrating our current knowledge of volatile hydroxides and oxyhydroxides. Blue shade indicates the metal hydroxides/oxyhydroxides are well characterized, green shade indicates reasonably known, and pink shade indicates data are needed.

https://doi.org/10.1557/jmr.2018.425 Published online by Cambridge University Press

© Materials Research Society 2019

methods, and free jet expansion mass spectrometry and the more novel steam jet method—are continually improving. The major limitation with transpiration is the analytical method for accurate determination of the deposit amount. As discussed, free jet expansion mass spectrometry has the potential to be quantitative if the gas dynamics are better understood in addition to the ionization and detection process. Evidence suggests that the steam jet method attains equilibrium for many systems and this needs to be clarified for all systems.

Conclusions

Reaction of water vapor with metal or metal oxide surfaces is an area of research with significant impact on several modern technologies. Accurate thermodynamic data are necessary to determine the suitability of specific materials in contact with water vapor at elevated temperatures and to accurately predict lifetimes. Such data can be put into the databanks of thermochemical modeling codes, such as FactSage [57]. A number of oxides have been studied, but additional data are definitely needed. Silicon, aluminum, and chromium compounds have been characterized, but a number of transition metal oxides warrant additional study. In particular, the yttrium and titanium systems are of importance.

The best approach is to combine experimental measurements with computational studies. Transition metals are more challenging with their large numbers of electrons, but modern computational techniques are making such studies more accurate and feasible all the time.

Free jet expansion mass spectrometry provides a way to identify volatile hydroxides and oxyhydroxides. Structures can be determined by spectroscopic techniques in conjunction with matrix isolation. Computational methods can provide a useful check on experimental results or provide reasonable structures when spectroscopic data are unavailable. Transpiration experiments can provide accurate thermodynamic data, especially when coupled with gefs obtained from spectroscopy or computation. Composite computational techniques provide invaluable checks on experimental results. Thermogravimetric analysis or steam jet experiments provide an important simulation of laminar or turbulent flow conditions typically found in actual applications. Examples of recent studies are discussed. Needed data for other systems are discussed as well as improvements to the theoretical and experimental techniques employed.

References

1. **O. Glemser and H.G. Wendlandt**: Gaseous hydroxides. In *Advances in Inorganic Chemistry and Radiochemistry*, Vol. **5**, H.J. Emeléus and A.G. Sharpe, eds., pp. 215–258 (Academic Press, New York, 1963).
2. **J.W. Hastie**: *High Temperature Vapors Science and Technology* (Academic Press, New York, 1975); pp. 60–87.
3. **P.J. Meschter, E.J. Opila, and N.S. Jacobson:** Water vapor mediated volatilization of high temperature materials. In *Annual Reviews of Materials Research*, D.M. Lipkin, ed. (Annual Reviews, Inc., Palo Alto, 2013).
4. **N.S. Jacobson**: High-temperature durability considerations for HSCT combustor. NASA TP-3162 (1992).
5. **I. Glassman**: *Combustion*, 2nd ed. (Academic Press, Inc., Orlando, 1987).
6. **E.J. Opila and D.L. Myers**: Alumina volatility in water vapor at elevated temperatures. *J. Am. Ceram. Soc.* **87**, 1701–1705 (2004).
7. **E.J. Opila and D.L. Myers:** Alumina volatility in water vapor at elevated temperatures: Application to combustion environments. In *High Temperature Corrosion and Materials Chemistry IV*, E. Opila, P. Hou, T. Maruyama, B. Pieraggi, D. Shifler, and E. Wuchina, eds. (The Electrochemical Society, Inc., Pennington, New Jersey, 2003); pp. 535–544.
8. **J.W. Fergus**: Effect of cathode and electrolyte transport properties on chromium poisoning in solid oxide fuel cells. *Int. J. Hydrogen Energy* **32**, 3664–3671 (2007).
9. **D.J. Young and B.A. Pint**: Chromium volatilization rates from Cr_2O_3 scales into flowing gases containing water vapor. *Oxid. Met.* **66**, 137–153 (2006).
10. **A. Kantrowitz and J. Grey**: A high intensity source for the molecular beam. I. Theoretical. *Rev. Sci. Instrum.* **21**, 328 (1951).
11. **T.A. Milne and F.T. Greene:** Direct mass spectrometric sampling of high pressure systems. In *Mass Spectrometry in Inorganic Chemistry*, J.L. Margrave, ed. (ACS, Washington DC, 1968); ch. 5, pp. 68–82.
12. **C.A. Stearns, F.J. Kohl, G.C. Fryburg, and R.A. Miller**: *A High Pressure Modulated Molecular Beam Mass Spectrometric Sampling System: NASA Technical Memorandum 73720* (National Aeronautics and Space Administration, Washington, DC, 1977).
13. **E.J. Opila, D.S. Fox, and N.S. Jacobson**: Mass spectrometric identification of Si–O–H(g) species from the reaction of silica with water vapor at atmospheric pressure. *J. Am. Ceram. Soc.* **80**, 1009–1012 (1997).
14. **D.L. Myers and N.S. Jacobson**: Identification of volatile metal hydroxides with free jet expansion mass spectrometry. In *Proceedings of International KEMS Workshop*, D. Kobertz, N. Jacobson, and D. Sergeev, eds., *Calphad* Special Issue, in press (Juelich, Germany, 2017).
15. **D. Myers, M. Kulis, J. Horvath, N. Jacobson, and D. Fox**: Interactions of Ta_2O_5 with water vapor at elevated temperatures. *J. Am. Ceram. Soc.* **100**, 2353–2357 (2017).
16. **G.C. Fryburg, R.A. Miller, F.J. Kohl, and C.A. Stearns**: Volatile products in the corrosion of Cr, Mo, Ti, and four superalloys exposed to O_2 containing H_2O and gaseous NaCl. *J. Electrochem. Soc.* **124**, 1738–1743 (1977).
17. **J.W. Hastie, K.F. Zmbov, and D.W. Bonnell**: Transpiration mass spectrometric analysis of liquid KCl and KOH vaporization. In

https://doi.org/10.1557/jmr.2018.425 Published online by Cambridge University Press

© Materials Research Society 2019

Modern High Temperature Science, J.L. Margrave, ed. (Humana Press, Totowa, NJ, 1984); pp. 333–364.

18. **E.J. Opila, D.L. Myers, N.S. Jacobson, I.M.B. Nielsen, D.F. Johnson, J.K. Olminsky, and M.D. Allendorf**: Theoretical and experimental investigation of the thermochemistry of $CrO_2(OH)_2$(g). *J. Phys. Chem. A* **111**, 1971–1980 (2007).
19. **J.M. Bassler and J.L. Margrave:** High-temperature applications of infrared spectroscopy. In *The Characterization of High Temperature Vapors*, J.L. Margrave, ed. (John Wiley & Sons, Inc., New York, 1967); pp. 264–281.
20. **W. Weltner, Jr.**: The matrix-isolation technique applied to high temperature molecules. In *Advances in High Temperature Chemistry*, Vol. **2**., L. Eyring, ed. (Elsevier, New York, 1969); pp. 85–105.
21. **X. Wang and L. Andrews**: Infrared spectroscopic observations of the group 13 metal hydroxides, $M(OH)_{1,2,3}$ (M = Al, Ga, in, and Tl) and $HAl(OH)_2$. *J. Phys. Chem. A* **111**, 1860–1868 (2007).
22. **X.F. Wang and L. Andrews**: Infrared spectra for group 4 dihydroxide and tetrahydroxide molecules. *J. Phys. Chem. A* **109**, 10689–10701 (2005).
23. **L. Shao, L. Zhang, M. Chen, H. Lu, and M. Zhou**: Reactions of titanium oxides with water molecules. A matrix isolation FTIR and density functional study. *Chem. Phys. Lett.* **343**, 178–184 (2001).
24. **J.H. Jensen**: *Molecular Modeling Basics* (CRC Press, Boca Raton, 2010).
25. **U. Merton and W.E. Bell: The transpiration method.** In *The Characterization of High Temperature Vapors*, J.L. Margrave, ed. (John Wiley & Sons, Inc., New York, 1967); p. 91.
26. **G.R. Belton and F.D. Richardson**: A volatile iron hydroxide. *Trans. Faraday Soc.* **58**, 1562–1572 (1962).
27. **G.R. Belton and R.L. McCarron**: The volatilization of tungsten in the presence of water vapor. *J. Phys. Chem.* **68**, 1852–1856 (1964).
28. **G.R. Belton and A.S. Jordan**: The volatilization of molybdenum in the presence of water vapor. *J. Phys. Chem.* **69**, 2065–2071 (1965).
29. **G.R. Belton and A.S. Jordan**: The gaseous hydroxides of cobalt and nickel. *J. Phys. Chem.* **71**, 4114–4120 (1967).
30. **Y.W. Kim and G.R. Belton**: The thermodynamics of volatilization of chromic oxide: Part I. The species CrO_3 and CrO_2OH. *Metall. Trans.* **5**, 1811–1816 (1974).
31. **A. Hashimoto**: The effect of H_2O gas on volatilities of planet forming major elements: I. Experimental determination of thermodynamic properties of Ca-, Al-, and Si-hydroxide gas molecules and its application to the solar nebula. *Geochim. Cosmochim. Acta* **56**, 511–532 (1992).
32. **N.S. Jacobson, E.J. Opila, D.L. Myers, and E.H. Copland**: Thermodynamics of gas phase species in the Si–O–H system. *J. Chem. Thermodyn.* **37**, 1130–1137 (2005).
33. **J. Drowart and P. Goldfinger**: Investigation of inorganic systems at high temperature by mass spectrometry. *Angew. Chem., Int. Ed.* **6**, 581–596 (1967).
34. **E.J. Opila, J.L. Smialek, R.C. Robinson, D.S. Fox, and N.S. Jacobson**: SiC recession caused by SiO_2 scale volatility under combustion conditions: II, thermodynamics and gaseous-diffusion model. *J. Am. Ceram. Soc.* **82**, 1826–1834 (1999).
35. **O.H. Krikorian**: Thermodynamics of the silica-steam system. In *Symposium on Engineering with Nuclear Explosives* (Las Vegas, Nevada, 1970). (unpublished).
36. **C.L. Darling and H.B. Schlegel**: Heats of formation of SiH_nO and SiH_nO_2 calculated by ab initio molecular orbital methods at the G-2 level of theory. *J. Phys. Chem.* **97**, 8207–8211 (1993).
37. **M.D. Allendorf, C.F. Melius, P. Ho, and M.R. Zachariah**: Theoretical study of the thermochemistry of molecules in the Si–O–H system. *J. Phys. Chem.* **99**, 15285–15293 (1995).
38. **A.V. Plyasunov**: Thermodynamic properties of H_4SiO_4 in the ideal gas state as evaluated from experimental data. *Geochim. Cosmochim. Acta* **75**, 3853–3865 (2011).
39. **L.V. Gurvich, I.V. Veyts, and C.B. Alcock**: Thermodynamic properties of individual substances: Elements O, H (D, T), F, Cl, Br, I, He, Ne, Ar, Kr, Xe, Rn, S, N, P and their compounds. Pt. 1. Methods and computation. Pt. 2. Tables. Vol. 1–2. Hemisphere, (1989) and Vol. 3, Begell House, Inc., New York (1989).
40. **B.B. Ebbinghaus**: Thermodynamics of gas phase chromium species: The chromium oxides, the chromium oxyhydroxides, and volatility calculations in waste incineration processes. *Combust. Flame* **93**, 119–137 (1993).
41. **M. Stanislowski, E. Wessel, K. Hilpert, T. Markus, and L. Singheiser**: Chromium Vaporization from High Temperature Alloys I. Chromia-Forming Steels and the Influence of Outer Oxide Layers. *J. Electrochem. Soc.* **154**, A295–A306 (2007).
42. **Q.N. Nguyen, D.L. Myers, N.S. Jacobson, and E.J. Opila**: Experimental and theoretical study of the reactions of titania and water at high temperatures. NASA/TM—2014-218372 (2014).
43. **Q.N. Nguyen, C.W. Bauschlicher, Jr., D.L. Myers, N.S. Jacobson, and E.J. Opila**: Computational and experimental study of thermodynamics of the reaction of titania and water at high temperatures. *J. Phys. Chem. A* **121**, 9508–9517 (2017).
44. **G.H. Geiger and D.R. Poirer**: *Transport Phenomena in Metallurgy*, Vol. **532** (Addison-Wesley Publishing Co., Reading, Massachusetts, 1972).
45. **S.L. dos Santos e Lucato, O.H. Sudre, and D.B. Marshall**: A method for assessing reactions of water vapor with materials in high-speed, high-temperature flow. *J. Am. Ceram. Soc.* **94**, 186–195 (2011).
46. **R.A. Golden and E.J. Opila**: A method for assessing the volatility of oxides in high-temperature high velocity vapor. *J. Eur. Ceram. Soc.* **36**, 1135–1147 (2016).
47. **K.A. Mueller, R.A. Golden, and E.J. Opila**: High temperature behavior of Ta_2O_5 in water vapor. *The Spectra*, **IX**, 50–55 (2018).
48. **O.H. Krikorian**: Predictive calculations of volatilities of metals and oxides in steam containing environments. *High Temp.-High Pressures* **14**, 387–397 (1982).
49. **F.T. Greene: Applications of electronic spectroscopy to high-temperature systems. In *The Characterization of High Temperature Vapors*, J.L. Margrave**, ed. (John Wiley & Sons, New York, 1967); pp. 300–358.

https://doi.org/10.1557/jmr.2018.425 Published online by Cambridge University Press

© Materials Research Society 2019

50. **M.W. Chase, Jr.**: *NIST-JANAF Thermochemical Tables*, 4th ed. Published by the American Chemical Society, the American Institute of Physics, and the National Institute of Standards and Technology. J. Phys. Chem. Ref. Data, Monograph No. 9 (1998).
51. **A.V. Plyasunov, A.S. Zyubin, and T.S. Zyubina**: Thermodynamic properties of $Si(OH)_4(g)$ based on experimental and quantum chemistry data. *J. Am. Ceram. Soc.* **101**, 4921–4926 (2018).
52. **J.M.L. Martin**: Basis set convergence and performance of density functional theory including exact exchange contributions for geometries and harmonic frequencies. *Mol. Phys.* **86**, 1437 (1995).
53. **A.P. Scott and L. Radom**: Harmonic vibrational frequencies: An evaluation of Hartree–Fock, moller–Plesset, quadratic configuration interaction, density functional theory, and semiempirical scale factors. *J. Phys. Chem.* **100**, 16502–16513 (1996).
54. **K.S. Pitzer and W.D. Gwinn:** Energy levels and thermodynamic functions for molecules with internal rotation: I. Rigid frame with attached tops. In *Molecular Structure and Statistical Thermodynamics*: Selected Papers of, Kenneth S. Pitzer, ed. (World Scientific, Singapore, 1993); pp. 33–46.
55. **E. Courcot, F. Rebillat, F. Teyssandier, and C. Louchet-Pouillerie**: Stability of rare earth oxides in a moist environment at high temperatures—Experimental and thermodynamic studies. Part I: The way to assess thermodynamic parameters from volatilisation rates. *J. Eur. Ceram. Soc.* **30**, 1903–1909 (2010).
56. **E. Courcot, F. Rebillat, F. Teyssandier, and C. Louchet-Pouillerie**: Stability of rare earth oxides in a moist environment at elevated temperatures—Experimental and thermodynamic studies: Part II: Comparison of the rare earth oxides. *J. Eur. Ceram. Soc.* **30**, 1911–1917 (2010).
57. **C.W. Bale, P. Chartrand, S.A. Degterov, G. Eriksson, K. Hack, R.B. Mahfoud, J. Melançon, A.D. Pelton, and S. Petersen**: FactSage thermochemical software and databases. *Calphad* **26**, 189–228 (2002).

https://doi.org/10.1557/jmr.2018.425 Published online by Cambridge University Press

© Materials Research Society 2019